

INTERNATIONAL SOCIETY FOR SOIL MECHANICS AND GEOTECHNICAL ENGINEERING



This paper was downloaded from the Online Library of the International Society for Soil Mechanics and Geotechnical Engineering (ISSMGE). The library is available here:

<https://www.issmge.org/publications/online-library>

This is an open-access database that archives thousands of papers published under the Auspices of the ISSMGE and maintained by the Innovation and Development Committee of ISSMGE.

The paper was published in the proceedings of the 10th European Conference on Numerical Methods in Geotechnical Engineering and was edited by Lidija Zdravkovic, Stavroula Kontoe, Aikaterini Tsiampousi and David Taborda. The conference was held from June 26th to June 28th 2023 at the Imperial College London, United Kingdom.

To see the complete list of papers in the proceedings visit the link below:

<https://issmge.org/files/NUMGE2023-Preface.pdf>

Numerical assessment of drilling-induced static liquefaction triggering of Feijão Dam I

A. Arenas¹, D. Reid², R. Fanni³, K. Smith³, A. Fourie²

¹Red Earth Engineering, a Geosyntec company, Perth, Australia

²The University of Western Australia, Perth, Australia

³WSP Golder, Perth, Australia

ABSTRACT: Dam I at Vale's Córrego do Feijão Iron Ore Mine dam failed on 25 January 2019, resulting in over 250 fatalities and catastrophic economic and environmental damage. Two major investigations have thus far been carried out to investigate the likely triggering event for the failure, leading to different conclusions: (a) a combination of reduction in near-surface suction and drained creep, or (b) liquefaction induced by drilling works occurring at the time of the failure. Other research works published subsequently have suggested either trigger is plausible. The current work reanalysed the liquefaction triggering process to assess whether drilling works, at two sections, could trigger liquefaction first in the immediate area around the borehole by leading to an increase in pore water pressure around the drill hole and then whether this would be sufficient to lead to flow liquefaction of the entire structure. This paper outlines preliminary two dimensional liquefaction triggering analyses of the tailings storage facility (TSF), with the sections representing the location of borehole drilling at the time of the failure and the immediately preceding location. The analyses indicated that the triggering of flow liquefaction was more likely at the location of borehole drilling concurrent with the dam failure, and less likely with the previous borehole drilling. These results are consistent with the observed failure.

Keywords: Feijão; flow liquefaction; triggering analysis; state parameter

1 INTRODUCTION

Dam I at Vale's Córrego do Feijão Iron Ore Mine dam failed on 25 January 2019, resulting in over 250 fatalities and significant economic and environmental damage. The devastating consequences of this failure, coupled with other catastrophic tailings storage facility (TSF) failures that have occurred during the past decade, has driven significant efforts to improve the safety of TSFs (ICOLD 2022, Morrison 2022).

Distinct from the tragic outcomes of the failure and the clear visual evidence of flow liquefaction provided by video of the failure, there remains significant debate as to the triggering event for the failure. Two major investigations of the failure have been carried out to date:

- The Expert Panel (EP) on the Technical Causes of the Failure of Feijão Dam I, retained by the law firm Skadden, Arps, Slate, Meagher and Flom LLP (legal counsel Vale), published a report in December 2019 (Robertson et al. 2019). This group identified a combination of reducing surficial suction (through increased rainfall) and drained creep as the proximate triggers for the failure. Drilling activities un-

derway at the time of the failure were explicitly stated as not being a plausible cause of the failure by this group.

- CIMNE, retained by the Federal Prosecutor's Office of Brazil, published a report in August 2021 (Arroyo and Gens 2021). This group identified drilling-induced liquefaction as the proximate trigger for the failure. Creep and reduction in suction were explicitly stated as not being a plausible cause of the failure by this group.

Clearly, significant differences of opinion exist between the two investigations thus far carried out to examine the failure. Subsequent analyses of the TSF published for the purpose of research have either stated that they were not focussed on the proximate triggers (Whittle et al. 2022) or have found that either of the two hypotheses outlined by the different investigators were plausible (Oathes and Boulanger 2022). Finally, summaries of the initial investigation prepared for Vale have argued that it may never be possible to determine what, if any, proportion of the failure triggering was a result of the drilling works (CIAEA 2020).

Given the current lack of consensus on the proximate trigger of the Feijão failure, the current paper outlines

the early development of geometry, in situ state, and initial 2D triggering assessments of the TSF carried out to critically appraise the potential for drilling works to have contributed to the failure. This forms part of a larger project to reassess the failure, with full 3D analysis building on the preliminary analyses outlined herein.

2 BACKGROUND

The numerical analysis procedures and inputs adopted by the previous investigations are first outlined as background. The methods broadly consistent between the two groups were as follows:

- Inferring state parameter (Ψ) for the tailings based on CPTu results using common current techniques (Plewes et al. 1992, Robertson 2010, Shuttle and Jefferies 2016)
- Strengths for the tailings were based largely on reconstituted triaxial compression tests on specimens prepared using moist tamping, with strength values and/or trends interrogated in the context of state parameter.
- Delineating the tailings into material types in areas of relevance to stability (i.e. below and near to the slope) based on CPTu results, with the EP adopting coarse and fine tailings groupings, while CIMNE adopted coarse, fine, and “mixtures”. Slimes were identified by both groups further back from the slope in locations that did not have an impact on the stability of the TSF.

The remaining techniques adopted by the two groups differ substantially, with the different approaches taken outlined as follows:

- Constitutive model
 - EP: Primary analyses were carried out using a user-input strain weakening relationship, where the peak and residual strength values and stiffness values were made functions of Ψ .
 - CIMNE: the Clay and Sand Model (CASM: Yu 1998) was adopted, being calibrated for coarse, fine, and tailings mixtures based on inferred characteristic Ψ values for each of the materials.
- In situ Ψ /strength delineation:
 - EP developed statistical distributions of Ψ for coarse and fine tailings and applied these stochastically to the model using the Local Area Subdivision approach. Forty different models were prepared, and the susceptibility of each model to failure was carried out through a strength reduction method (SRM) factor of safety (FoS) calculation obtained through reduction of peak strengths to detect failure. This indicated the 40 models produced FoS ranging from ~0.5 to 2.0. Four models with FoS results of 1.0 to 1.2 were adopted for subsequent triggering analyses.
 - CIMNE: Each of the inferred zones of coarse, fine, and mixtures, were assigned the same CASM

input parameters – e.g. all coarse tailings in the model would exhibit similar strengths.

- Geometry
 - EP carried out analyses in 3D
 - CIMNE carried out analyses in 2D and as “pseudo-3D”, where 15m wide models were created by extruding 2D sections.

3 NUMERICAL MODEL DEVELOPMENT

3.1 Analysis framework

The analysis framework adopted to examine the potential triggering of flow liquefaction at the Feijão TSF was based on the work of Reid et al. (2021). This work outlined a simplified procedure to examine all elements of saturated tailings within a numerical model, examine if in situ stress ratio η (ratio between the deviatoric stress, q , and the mean effective stress, p') was greater than an instability value η_{IL} at any locations, and if so assign liquefied strengths to triggered elements, reassess stability, and continue this process iteratively to assess if the model would converge. This framework was adopted as it is amenable to the analysis of a constant shear drained (CSD) stress path as may occur around a borehole owing to increased pore pressures for what was clearly a brittle, loose tailings. Although, the authors are not aware of an analogous failure in the literature where borehole drilling may have triggered CSD failure, several examples of this trigger mechanism are reported due to phreatic surface rise, e.g. Aberfan tip (Bishop 1966, Jefferies and Been 2015), Wachusett Dam (Olson et al. 2000), Stava TSF (Morgenstern 2001) and Edenville-Sandford Dam (France et al. 2021).

Two 2D sections were analysed in FLAC3D, referred to as SM09 and SM13. These sections were selected to pass through the final two boreholes advanced at the TSF prior to the failure, both on the same bench. These are analysed and compared to produce an initial assessment of the in situ conditions and stress state at each location/section. This comparison was an important first step in the work as one of the EP arguments against drilling being the proximate trigger was that previous drilling works did not cause failure. Examining and comparing these two sections allows an initial investigation as to whether the in situ state and stress conditions at the final borehole location (SM13) were such that triggering was more likely than the penultimate borehole location (SM09).

3.2 Geometry development

The numerical model geometry was developed from public information, primarily from the EP report. The public information regarding Feijão dam geometry and

local topography is comprised of plain images and tables. Plain images do not carry digital information, such as UTM coordinates or elevations.

The software Geo Meshing v4.2.1 was used to overcome the challenge of converting this information into the detailed 2D/3D numerical models. Geo Meshing uses parametric inputs (e.g. crest width) for creating 2D/3D meshes and it does not require 3D surfaces or 3D volumes. Geo Meshing was also used for the interpolation of Ψ within tailings elements, which were inferred from CPTu data.

The 3D model has 2.3 million elements, whereas each 2D model has approximately 80 thousand elements. At the refined model area, the element size is approximately 1.4 m high and 2.5 m wide. Figure 1 presents details of the 3D model, while Figure 2 shows the location of the two 2D sections.

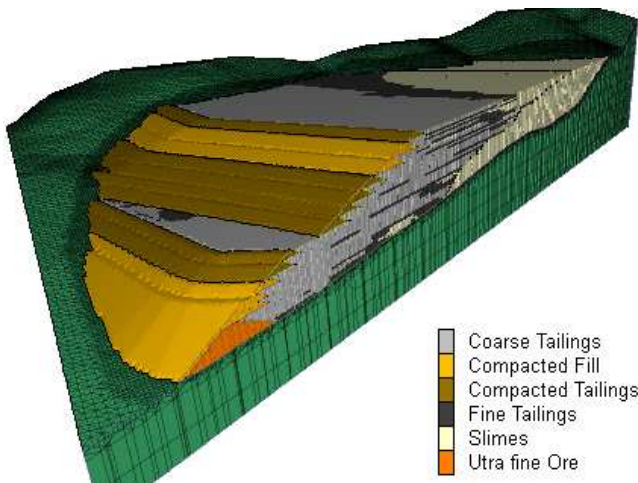


Figure 1. 3D Numerical Model. Model cut where borehole SM13 was being drilled on the day of the failure. The section shows the layering used during model construction.

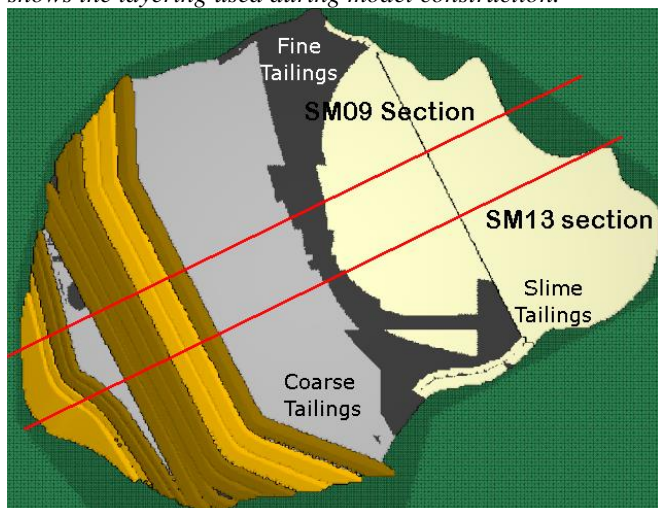


Figure 2. Plan of model showing 2D section locations.

3.3 Constitutive models

Each of the materials modelled were simulated using the Mohr Coulomb (MC) constitutive model (Itasca 2019), adopting the parameters outlined in Table 1.

Table 1. Constitutive model inputs

Material	Shear Modulus Reference ¹ (kPa)	Friction (°)	Cohesion (kPa)
Foundation	1,472,000*	N/A ²	N/A ²
Slimes	1,285	0	0.22(σ'_v)
Compacted Tailings	3,496	40	0
Compacted Fill	2,525	35	10
Ultra fine Ore	2,525	35	10
Fine Tailings	1,028	33.2	5
Coarse Tailings	1,028	34.6	5

Note¹ $G = G_0 P_a \left(\frac{p'}{P_a}\right)^n$, where G_0 is the Shear reference modulus. When denoted by *, it refers to the shear modulus. Note² Elastic constitutive model adopted.

While use of MC for stiff foundations or compacted embankments is not uncommon even in increasing advanced modelling efforts, the implementation of MC for a saturated, contractive, brittle tailings warrants further discussion.

The use of MC, in a modified form, for the tailings is based on the following rationale: (i) no constitutive model, to the author's knowledge, has been demonstrated to reliably capture behaviour on the CSD stress path in a boundary value problem for loose, contractive, brittle soils, (ii) use of any constitutive model, however advanced, leads to either an implicit or explicit assumption around the in situ values of K_0 , K_c , and Lode Angle that develop in situ – something not frequently acknowledged in published static liquefaction numerical analyses but of critical importance to identifying the initiation of instability when checking if $\eta > \eta_{IL}$ (either implicitly or explicitly).

To overcome the issues outlined above, the MC model was adopted with a value of Poisson's ratio selected to target a specified K_0 below level ground – this being 0.7 in this case. This allows a plausible value of in situ K_0 to be obtained, something not always the case in more advanced models. To identify the initiation of instability, the η in all elements can be tracked by means of routines prepared by the authors that scan all elements of the saturated tailings and assess whether $\eta > \eta_{IL}$. Liquefied strengths can then be applied to such elements as cohesion inputs, essentially switching the failure criterion from MC to Tresca. We note that during the static construction, the MC strength criterion is not used as a review of the state of the materials indicated that there were no elements in the model in a plastic state, therefore the elastic input parameters of the model control the in situ stress state, while during the triggering process the modifications applied by the authors control instability and liquefied strength. This triggering analysis process is outlined in more detail subsequently.

3.4 Instability stress ratios

A crucial input to a triggering analysis of the form carried out herein is the η_{IL} value adopted for in situ tailings; specifically, the relationship between η_{IL} and Ψ (e.g. Yang 2002). To develop such a relationship for the Feijão tailings, the triaxial compression tests carried out by both investigation groups were synthesised as presented in Figure 3. Electronic data for CIMNE tests were available (Viana da Fonseca et al. 2022), however the EP tests were unable to be shared with the authors, therefore, previously digitised data (Reid et al. 2022) were utilised.

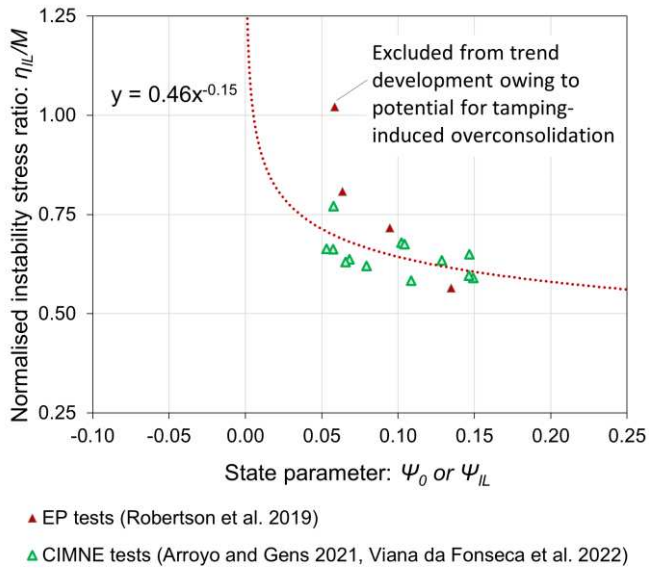


Figure 3. Development of normalised instability stress ratio – state parameter trend for use in analyses

The data presented in Figure 3 and the selected trend are normalised by M : in the case of the triaxial compression tests presented, this being M_{ic} . This form of normalisation allows the triaxial compression data to be plausibly extended to the in situ plane strain conditions of the numerical model. It is also noted that one of the tests carried out by the EP was excluded from the synthesis in Figure 3 (as annotated) owing to the potential for tamping-induced overconsolidation to have affected the resulting peak strength / η_{IL} (Reid et al. 2022).

It is noted that no suitable strength tests on the Feijão slimes were available for use in the framework of Figure 3 – an important limitation of the available data, given that it appears slimes may have been present at the base of BH SM13. Given this lack of information, the same trend as for fine/coarse tailings was adopted for the slimes, with the scaling based on the inferred lower M_{ic}/M for the slimes as outlined subsequently.

3.5 Liquefied strength ratios

Liquefied strength ratios for the tailings were based on the “best practice trends” proposed by Jefferies and Been (2015), where $s_u(liq)/\sigma'_{vc}$ is a function of Ψ , in-

formed through both the back analysis of flow liquefaction case histories and CSSM. This method is preferred to the “steady state approach” owing to the clear evidence of flow liquefaction of deposits with Ψ ranging from -0.05 to +0.05, behaviour inconsistent with the assumption of fully undrained conditions tending towards the CSL.

3.6 In situ state and tailings type distribution

As noted previously, both η_{IL} and $s_u(LIQ)/\sigma'_{vc}$ values used in the modelling are functions of Ψ . Thus, the interpretation of Ψ and the assumed distribution in situ are of critical importance to the outcomes of the analyses.

As previously mentioned, Ψ was interpolated from CPTu data using a built in feature of Geo Meshing v4.2.1. The interpolation scheme used a bin of 0.75 m height (half of the numerical element height) and 50% percentile Ψ values. Several bin sizes were tested, and the selected value provided the smallest mesh bias. Similarly, the 50% percentile appeared to provide a good field representation of Ψ , without being over conservative. Jefferies and Been (2015) recommend adoption of 80% Ψ when a single value is to represent the entire domain. However, as the present analysis is detailed to the numerical element level, adoption of 80% Ψ would result in overconservative system responses. Ψ was estimated from CPTu data using the Plewes et al. (1992) inversion method. Figure 4 shows the interpreted Ψ distribution for each section.

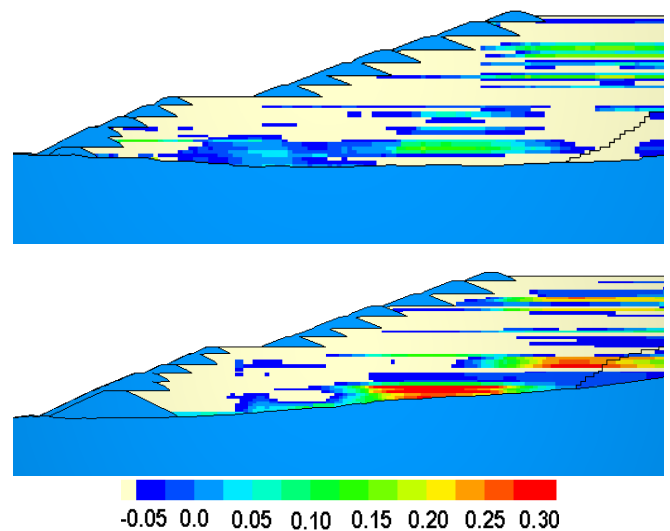


Figure 4. State parameter distribution. Above, section SM09. Below, section SM13.

3.7 Tailings placement and phreatic surface

The construction sequence simulation of Feijão TSF was grouped in 13 stages. Each stage was subdivided in layers of about 1.5 m. This subdivision produced 78 lifts for the embankment raises and 53 lifts for the tailings. The lifts were sequentially and alternately activated to simulate the TSF construction. A K_0 of 0.7 was used

during construction of both sections. Although this might seem an arbitrary value, it provides numerical stability before testing the present methodology. Based on Figure 6, K_0 was selected such that in-situ stresses, for the most contractive materials, were as close as possible to the instability line, but below it.

The phreatic level was updated at the end of each construction stage. The phreatic level used for each stage was based on the seepage analysis performed by the EP.

3.8 Triggering assessment procedure

Once the model had been brought to equilibrium under the conditions previously described, an assessment of the potential for the triggering of instability around the boreholes during drilling was carried out. This process involved two major stages (i) establish a pore pressure regime around the borehole (Loop 1) and ii) Checking for triggering (Loop 2) as also illustrated in Figure 5. This represents a modified form of that adopted by Reid et al. (2021).

4 PRELIMINARY MODEL OUTCOMES

4.1 In situ stress state prior to drilling

Initial comparison of the trend line (Figure 3) vs in situ Ψ was performed for section SM09 and SM13. The information was gathered from the full 3D model over 10 m width at each section. Figure 6 shows how the insitu conditions at borehole SM13 is more susceptible to triggering, given the closer proximity to the instability trend line. This may help explain why drilling borehole SM09 did not trigger failure of the TSF.

4.2 Stability of 2D section after drilling

Figures 7 and Figure 8 show the analysis results. The upper portion of each figure presents the horizontal displacements in meters. The plot has been capped at 2 m to more clearly present small displacements. The middle plot shows liquefied zones (zones with $\eta > \eta_{IL}$). The lower plot shows shear strain, capped to a maximum value of 30%.

It should be noted that consistent triggering mechanisms, pore water pressure magnitudes and flow schemes, and Ψ interpolation schemes have been applied to both sections.

It is evident that section SM09 does not develop instability under the imposed conditions. On the other hand, section SM13 develops significant deformations and strains, representing slope failure. As the models were run to large strains, it is possible to identify the surface settlement upstream of the crest and the bulging at the starter dam face (observed during failure) in Figure 8.

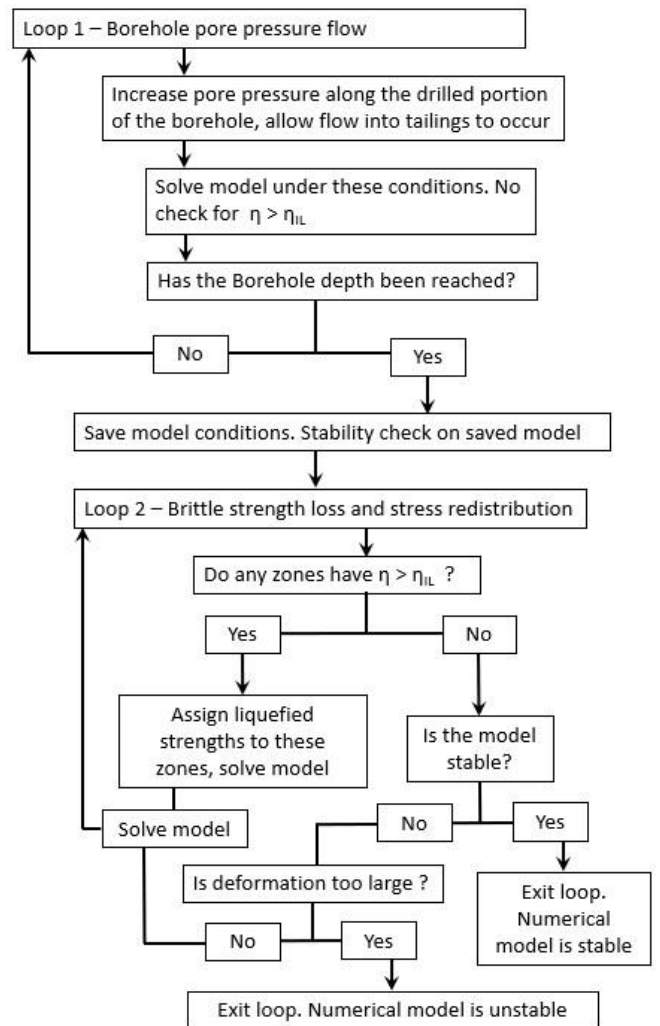


Figure 5. Flow diagram showing triggering assessment and stability analysis procedure.

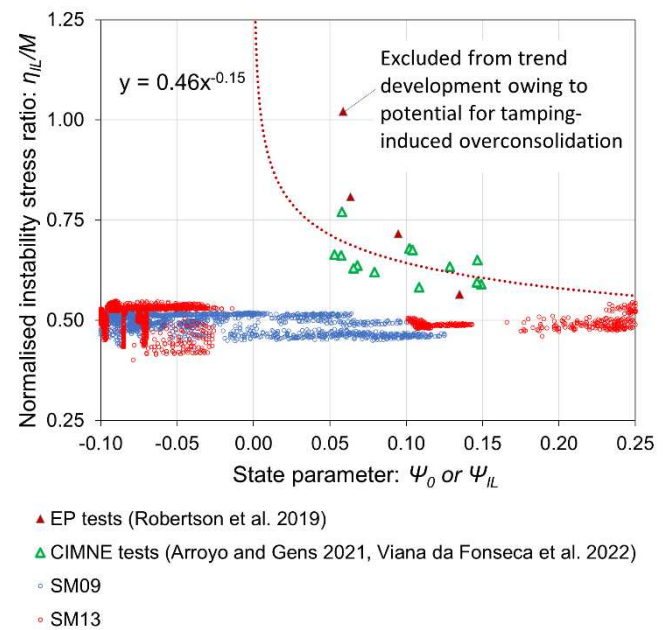


Figure 6. Normalized Instability stress ratio versus state parameter.

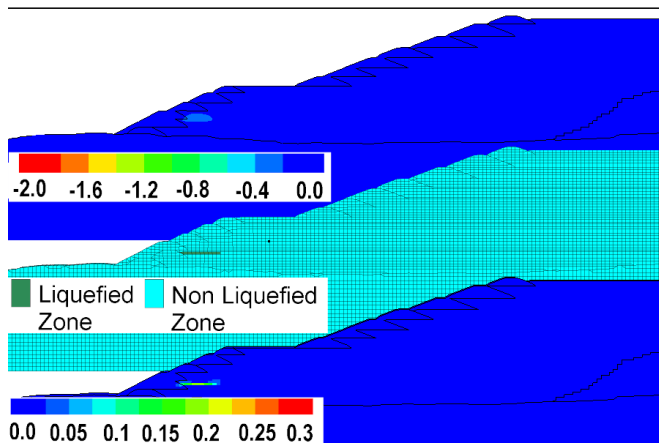


Figure 7. Section SM09. Upper, horizontal displacements. Middle, liquefied zones. Lower, shear strain.

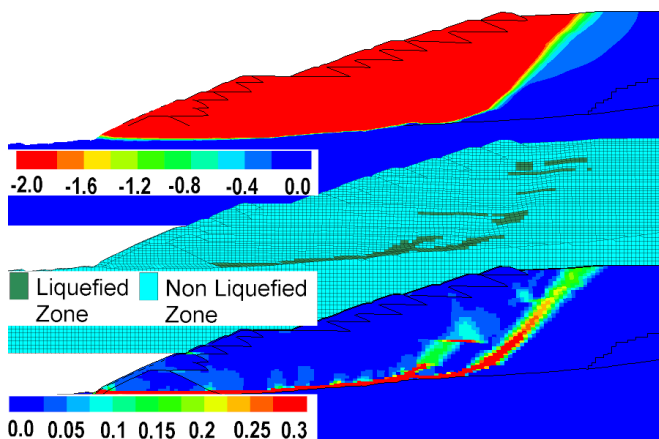


Figure 8. Section SM13. Upper, horizontal displacements. Middle, liquefied zones. Lower, shear strain.

5 CONCLUSIONS

The following conclusions can be drawn from the present work:

- The authors believe that the most plausible triggering mechanism for the Feijão TSF failure was the pore pressure induced by drilling of borehole SM13.
- The current analysis and methodology, based on Reid et al. (2021), aids in understanding why the TSF failed while drilling borehole SM13 and not while drilling borehole SM09.
- The methodology adopted provides a practical framework for the analysis and prediction of liquefaction triggering mechanisms.
- At the time of writing this paper, the authors were working on completing numerical modeling for the full 3D TSF. Results of the analyses will be presented in a separate paper.

REFERENCES

- Arroyo M, Gens A. 2021. Computational analyses of Dam I at the Corrego de Feijao mine in Brumadinho - Final Report. .
- Bishop AW. 1966. Sixth Rankine Lecture: The strength of soils as engineering materials. *Geotechnique* 16: 89–130.
- Extraordinary Independent Consulting Committee for Investigation (CIAEA). 2020. Executive Summary of the Independent Investigation Report, Failure of Dam 1 of the Córrego do Feijão Mine – Brumadinho, MG. .
- France JW, Alvia I, Williams JL, Miller A, Higinbotham S. 2021. Investigation of failures of Edenville and Sandford Dams - Interim Report. .
- Geo Meshing. 2022. v4.2.1. www.geomeshing.com
- ICOLD. 2022. Tailings Dam Safety Bulletin - Draft. .
- Itasca. 2019. FLAC3D manual.
- Jefferies M, Been K. 2015. *Soil Liquefaction: A Critical State Approach*, Second Edition. CRC Press.
- Morgenstern N. 2001. Geotechnics and mine waste management - update. Seminar on safe tailings dam construction. p. 54–67.
- Morrison KF. 2022. *Tailings Management Handbook: A LifeCycle Approach*. Society for Mining, Metallurgy & Exploration.
- Oathes TJ, Boulanger RW. 2022. Nonlinear viscoplastic modeling of the feijão dam 1 failure. *Geo-Congress 2022*.
- Olson SM, Stark TD, H. WW, Castro G. 2000. 1907 Static Liquefaction Flow Failure of the North Dike of Wachusett Dam. *Journal of Geotechnical and Geoenvironmental Engineering* 126: 1184–1193.
- Plewes HD, Davies MP, Jefferies MG. 1992. CPT based screening procedure for evaluation liquefaction susceptibility. 45th Canadian Geotechnical Conference. p. 41–49.
- Reid D, Dickinson S, Mital U, Fanni R, Fourie A. 2021. On some uncertainties related to static liquefaction triggering assessments. *Proceedings of the Institution of Civil Engineers - Geotechnical Engineering In Press*: .
- Reid D, Fanni R, Fourie A. 2022. Effect of Tamping Conditions on the Shear Strength of Tailings. *International Journal of Geomechanics* 22: 04021288.
- Robertson PK. 2010. Estimating in-situ state parameter and friction angle in sandy soils from the CPT. 2nd International Symposium on Cone Penetration Testing.
- Robertson PK, de Melo L, Williams DJ, Wilson GW. 2019. Report of the Expert Panel on the technical causes of the Failure of Feijão Dam I. .
- Shuttle D, Jefferies M. 2016. Determining silt state from CPTu. *Geotechnical Research* 3: 90–118.
- Viana da Fonseca A, Cordeiro D, Molina-Gómez F, Besenon D, Fonseca A, Ferreira C. 2022. The mechanics of iron tailings from laboratory tests on reconstituted samples collected in post-mortem Dam I in Brumadinho. *Soils and Rocks* 45: 1–20.
- Whittle AJ, El-Nagger HM, Sherif, A.Y.A., Abdullah, M.G. 2022. Stability Analysis of Upstream Tailings Dam Using Numerical Limit Analyses. *Journal of Geotechnical and Geoenvironmental Engineering* 148: 04022035.
- Yang J. 2002. Non-uniqueness of flow liquefaction line for loose sand. *Géotechnique* 52: 757–760.
- Yu HS. 1998. CASM: a unified state parameter model for clay and sand. *International Journal for Numerical and Analytical Methods in Geomechanics* 22: 621–653.